# CLASSIFICATION BASED ON THE POLARIMETRIC DISPERSIVE AND ANISOTROPIC BEHAVIOR OF SCATTERERS

*M. Duquenoy*[†‡], *J.P. Ovarlez*[†], *L. Vignaud*[†], *L. Ferro-Famil*[‡], *E. Pottier*[‡]

†: Signal Processing Unit, Electromagnetism and Radar Department (DEMR) ONERA, Palaiseau, France
Chemin de la Huniere, F-91761 Palaiseau cedex
Telephone: (+33) 1 69 93 62 95, Fax: (+33) 1 69 93 62 69
Email : mickael.duquenoy@onera.fr, ovarlez@onera.fr, vignaud@onera.fr
‡: Image and Remote Sensing Group, Institute of Electronics and Telecommunications from Rennes (IETR)
University of Rennes 1, Rennes, France
Campus Beaulieu, Bat 11D, 263 avenue General Leclerc, CS-74205 Rennes cedex
Telephone: (+33) 2 23 23 67 14, Fax: (+33) 2 23 23 69 63
Email : laurent.ferro-famil@univ-rennes1.fr, eric.pottier@univ-rennes1.fr

**ABSTRACT**

Conventional radar imaging assumes that all the scatterers are considered as bright points (isotropic for all observation angle and white in the frequency band). Recent studies based on multidimensional Time-Frequency Analysis, describe the angular and frequency behavior of scatterers and show that they are anisotropic and dispersive. Another information source in radar imaging is the polarimetry. Studies based on multidimensional wavelet and coherent decompositions allow to represent the angular and frequency polarimetric behavior and show the non-stationarity of this behavior. The aim of this paper, is to propose a classification process based on this new information source.

## 1. CLASSICAL RADAR IMAGE FORMATION

The classical model used in radar imaging is the model of bright points (i.e. a target is considered as a set of independent sources which are isotropic for all directions of presentation and white in the frequency band) [1], [2]. Let $I(\vec{r})$ be the complex amplitude of the bright point located in $\vec{r} = (x, y)^T$. Under far field conditions, the complex backscattering coefficient for the whole target is then given by the in-phase summation of each reflector contribution:

$$H(\vec{k}) = \int I(\vec{r})\, e^{-2i\pi\vec{k}.\vec{r}}\, d\vec{r}. \tag{1}$$

The wave vector $\vec{k}$ is related to the frequency $f$ and to the direction $\theta$ of illumination (observation angle) by $\left|\vec{k}\right| = 2f/c$ and $\theta = \arg(\vec{k})$. After a Fourier Transform of (1), one can obtain the spatial repartition (image) $I(\vec{r})$ of the reflectors for a mean frequency (the center frequency) and for a mean angle of presentation:

$$I(\vec{r}) = \int H(\vec{k})\, e^{2i\pi\vec{k}.\vec{r}}\, d\vec{k}. \tag{2}$$

A full polarimetric radar is generally designed to transmit and receive microwave radiation which is horizontally polarized (H) or vertically polarized (V). The polarimetric generalization of the scattering coefficient is called the scattering matrix or Sinclair matrix:

$$[S] = \begin{bmatrix} S_{hh} & S_{hv} \\ S_{vh} & S_{vv} \end{bmatrix} \tag{3}$$

## 2. 2D TIME-FREQUENCY ANALYSIS

When a target is illuminated by a broad-band signal and/or for a large angular extent, it is realistic to consider that the amplitude spatial repartition $I(\vec{r})$ of the reflectors depends on frequency $f$ and on aspect angle $\theta$. This repartition depending on the wave vector $\vec{k}$, it will be noted in the following by $I(\vec{r}, \vec{k})$.

Such images can be built using the multidimensional continuous wavelet transform extended to two dimensions and are called hyperimages [3], [4], [5]:

$$I(\vec{r_0}, \vec{k_0}) = \int H(\vec{k})\, \Psi^*_{\vec{r_0},\vec{k_0}}(\vec{k})\, d\vec{k}\,. \tag{4}$$

where $\Psi_{\vec{r}_0,\vec{k}_0}(\vec{k})$ is a family of wavelet bases generated from the mother wavelet $\phi(k, \theta)$ localized around $(k, \theta) = (1, 0)$ and located spatially at $\vec{r} = \vec{0}$ according to:

$$\Psi_{\vec{r}_0,\vec{k}_0}(\vec{k}) = \frac{1}{k_0}\, e^{-2i\pi\vec{k}.\vec{r}_0}\, \phi\left(\frac{k}{k_0}, \theta - \theta_0\right). \tag{5}$$

The scattering matrix will now depend on frequency and on angle of presentation and is called hyper-scattering matrix:

$$[S](\vec{r}, \vec{k}) = \begin{bmatrix} S_{hh}(\vec{r}, \vec{k}) & S_{hv}(\vec{r}, \vec{k}) \\ S_{vh}(\vec{r}, \vec{k}) & S_{vv}(\vec{r}, \vec{k}) \end{bmatrix} \tag{6}$$

The span is generally defined as the sum of the squared modulus of each element of the matrix (3). The extended

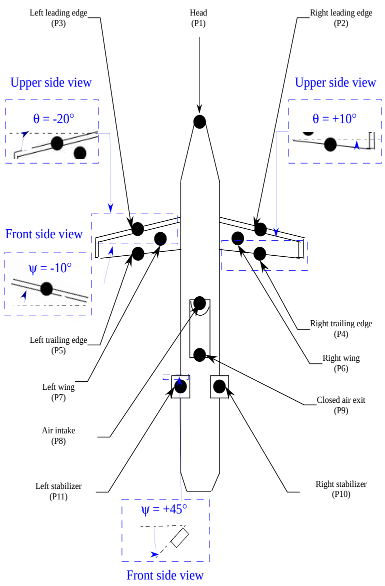


**Fig. 1**. The Cyrano weapon model.

span is now defined as the sum of the squared modulus of each element of the hyper-scattering matrix (6).

$$Span(\vec{r},\vec{k}) = |S_{hh}(\vec{r},\vec{k})|^2 + |S_{hv}(\vec{r},\vec{k})|^2 + |S_{vh}(\vec{r},\vec{k})|^2 + |S_{vv}(\vec{r},\vec{k})|^2. \quad (7)$$

The extended span has been tested on full polarimetric data from anechoic chamber between -25 and 25 degrees for a frequency band [12,18]GHz. The target is a "Cyrano" weapon model see fig 1..

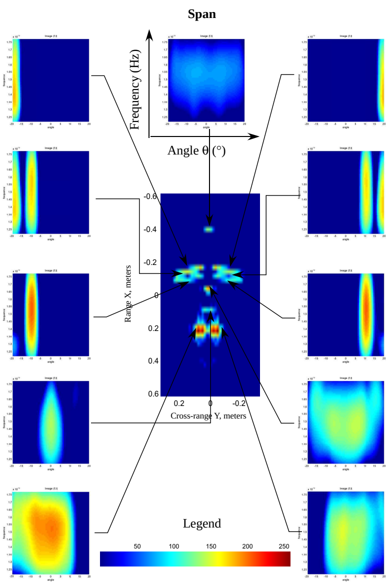


**Fig. 2**. Evolution of the span versus the emitted frequency and the illumination angle.

The span evolution of the cyrano weapon model shows that some scatterers are anisotropic and dispersive (see fig 2.).

## 3. CAMERON DECOMPOSITION

The aim of polarimetric coherent decompositions is to express the Scattering or Sinclair matrix (3) as a combination of the scattering responses of simpler objects [6]. The Cameron decomposition is based on two target properties: reciprocity and symmetry [7], [8].

A radar target is considered as reciprocal when the diagonal terms of the measured scattering matrix are equal i.e. the reciprocity theorem applies. For a scattering matrix measured in the orthogonal linear basis, it means, $S_{hv} = S_{vh}$ whereas for the orthogonal circular basis $S_{rl} = S_{lr}$. The reciprocity principle divides scattering matrix space into two subspaces, one containing only scattering matrices of reciprocal scatterers and the other only containing scattering matrices of non-reciprocal scatterers. A Sinclair matrix $[S]$ whose the associated vector is $\overrightarrow{S}$, is decomposed in the Pauli basis following:

$$\overrightarrow{S} = \begin{pmatrix} S_{hh} \\ S_{hv} \\ S_{vh} \\ S_{vv} \end{pmatrix} = \alpha\overrightarrow{S_a} + \beta\overrightarrow{S_b} + \gamma\overrightarrow{S_c} + \delta\overrightarrow{S_d} \quad (8)$$

$$[S]_a = \frac{1}{\sqrt{2}} \begin{bmatrix} 1 & 0 \\ 0 & 1 \end{bmatrix} \quad (9)$$

$$[S]_b = \frac{1}{\sqrt{2}} \begin{bmatrix} 1 & 0 \\ 0 & -1 \end{bmatrix} \quad (10)$$

$$[S]_c = \frac{1}{\sqrt{2}} \begin{bmatrix} 0 & 1 \\ 1 & 0 \end{bmatrix} \quad (11)$$

$$[S]_d = \frac{1}{\sqrt{2}} \begin{bmatrix} 0 & -1 \\ 1 & 0 \end{bmatrix} \quad (12)$$

So, the vector $\overrightarrow{S}$, can be expressed on the two subspaces defined by the reciprocity rule following:

$$\overrightarrow{S} = A\left(\cos(\theta_{rec})\,\overrightarrow{S}_{rec} + \sin(\theta_{rec})\,\overrightarrow{S}_{nr}\right) \quad (13)$$

where $\overrightarrow{S}_{rec}$ is the unit vector carrying the projection $P_{rec}$ of $\overrightarrow{S}$ on the reciprocal subspace.

$$\overrightarrow{S}_{rec} = P_{rec}\overrightarrow{S} \quad (14)$$

where $\overrightarrow{S}_{nr}$ is the nonreciprocal component of the vector $\overrightarrow{S}$. It is collinear to $\overrightarrow{S_d}$.

$$\overrightarrow{S}_{nr} = \frac{(\overrightarrow{S},\overrightarrow{S_d})}{|(\overrightarrow{S},\overrightarrow{S_d})|}\overrightarrow{S_d} \quad (15)$$

where $A$ is the norm of the vector $\overrightarrow{S}$.

$$A = ||\overrightarrow{S}|| \quad (16)$$

and where $\theta_{rec}$ represents the degree to which a scattering matrix obeys reciprocity. It is the angle between the scattering matrix and the reciprocal subspace.

$$\theta_{rec} = \cos^{-1}||P_{rec}\overrightarrow{S}|| \quad 0 \leq \theta_{rec} \leq \frac{\pi}{2} \quad (17)$$

Scattering matrices with $\theta_{rec} = 0$ correspond to scatterers which strictly obey the reciprocity principle. It is the case in SAR monostatic systems. Whereas scattering matrices with $\theta_{rec} = \frac{\pi}{2}$ lie entirely in the subspace orthogonal to the reciprocal subspace and hence violate the reciprocity principle.

A scattering is considered symmetric when the target has an axis of symmetry in the plane orthogonal to the direction between the radar and the target. The symmetry of a scatterer can be also considered in the frame of the Pauli decomposition. Hence, a scatterer is considered as symmetric if it exists a rotation of angle $\psi_d$, which cancels the projection of the vector $\overrightarrow{S}$ in the component $\overrightarrow{S_c}$ of the Pauli decomposition. A scattering matrix which corresponds to a reciprocal scatterer $\overrightarrow{S}_{rec}$ can be decomposed into a maximum symmetric component $\overrightarrow{S}^{sym}_{max}$ and a minimum symmetric component $\overrightarrow{S}^{sym}_{min}$:

$$\overrightarrow{S}_{rec} = \cos(\tau)\,\overrightarrow{S}^{sym}_{max} + \sin(\tau)\,\overrightarrow{S}^{sym}_{min} \qquad (18)$$

The angle $\tau$ represents the degree to which the reciprocal component of the scattering matrix deviates from belonging to the set of scattering matrices corresponding to symmetric scatterers:

$$\cos(\tau) = \frac{|(\overrightarrow{S}_{rec}, \overrightarrow{S}^{sym}_{max})|}{||\overrightarrow{S}_{rec}||\,||\overrightarrow{S}^{sym}_{max}||} \qquad (19)$$

A scattering matrix with $\tau = 0$ represents a fully symmetric scatterer such as a trihedral or dihedral, whereas a scattering matrix with $\tau = \frac{\pi}{4}$ represents a fully asymmetric scatterer such as a left helix or a right helix. Both vectors $\overrightarrow{S}^{sym}_{max}$ and $\overrightarrow{S}^{sym}_{min}$ are ideal symmetric scatterer scattering matrices. Minimum et maximum refer to the relative amplitude contributions of $\overrightarrow{S}^{sym}_{max}$ and $\overrightarrow{S}^{sym}_{min}$ to $\overrightarrow{S}_{rec}$. The projection of $\overrightarrow{S}_{rec}$ onto $\overrightarrow{S}^{sym}_{max}$ has a magnitude equal to $\cos(\tau)$ and the projection of $\overrightarrow{S}_{rec}$ onto $\overrightarrow{S}^{sym}_{min}$ has a magnitude equal to $\sin(\tau)$. A scatterer is considered as symmetric if $\tau$ has a value between 0 and $\frac{\pi}{4}$. By this fact, the magnitude of the projection onto $\overrightarrow{S}^{sym}_{max}$ is always greater than or equal to the magnitude of the projection onto $\overrightarrow{S}^{sym}_{min}$. $\overrightarrow{S}^{sym}_{max}$ is defined by:

$$\overrightarrow{S}^{sym}_{min} = \alpha\,\overrightarrow{S_a} + \varepsilon\,\overrightarrow{S_b} \qquad (20)$$

where $\varepsilon$ is given by:

$$\varepsilon = \beta\,\cos(\theta) + \gamma\,\sin(\theta) \quad \tan(2\theta) = \frac{\beta\gamma^* + \beta^*\gamma}{|\beta|^2 - |\gamma|^2} \qquad (21)$$

The Cameron decomposition expresses the Sinclair matrix $[S]$ as a sum of two symmetric components and a non-reciprocal component:

$$\overrightarrow{S} = A\left(\cos(\theta_{rec})\left(\cos(\tau)\,\overrightarrow{S}^{sym}_{max} + \sin(\tau)\,\overrightarrow{S}^{sym}_{min}\right) + \sin(\theta_{rec})\,\overrightarrow{S}_{nr}\right) \qquad (22)$$

An arbitrary symmetric scatterer $\overrightarrow{S}_{sym}$ can be decomposed according to:

$$\overrightarrow{S}_{sym} = a\,e^{i\rho}\,[R(\psi)]\,\overrightarrow{\Lambda}(z) \quad a \in R^+ \quad \rho, \psi \in (-\pi;\pi] \qquad (23)$$

where $a$ is the amplitude of the scattering matrix, $\rho$ is the nuisance phase and $\psi$ is the scatterer orientation angle (Huynen orientation). The matrix $[R(\psi)]$ denotes the rotation operator. Finally, the normalized vector $\overrightarrow{\Lambda}(z)$ expressed in the linear polarization basis is:

$$\overrightarrow{\Lambda}(z) = \frac{1}{\sqrt{1+|z|}}\begin{pmatrix}1\\0\\0\\z\end{pmatrix} \quad z \in C, |z| \leq 1 \qquad (24)$$

Consequently, the complex quantity $z$ can be used to characterize the symmetric scatterer under consideration. The following list presents the values of $z$ for some canonical targets.

| Symmetric Scatterer | Normalized Vector |
|---|---|
| Trihedral | $\overrightarrow{\Lambda}(1)$ |
| Diplane | $\overrightarrow{\Lambda}(-1)$ |
| Dipole | $\overrightarrow{\Lambda}(0)$ |
| Cylinder | $\overrightarrow{\Lambda}(\frac{1}{2})$ |
| Narrow Diplane | $\overrightarrow{\Lambda}(-\frac{1}{2})$ |
| Quarter Wave Device | $\overrightarrow{\Lambda}(i)$ |

**Table 1**. Examples of normalized vectors associated to some canonical scatterers.

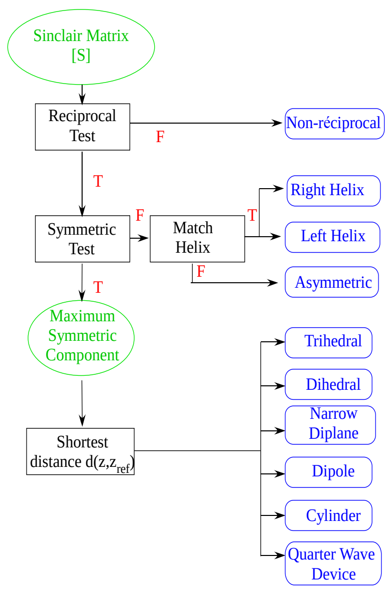


**Fig. 3**. Classification process of the Cameron decomposition.

On the basis of the factorization of the measured scattering matrix $[S]$, Cameron proposed a classification scheme for the Sinclair matrix (see fig 3.). The first decision to make is to choose if a scatterer is reciprocal or none. The characteristic parameter of this sort of measure is the angle $\theta_{rec}$. If it is lower than $\frac{\pi}{4}$ we will take the decision that the scatterer is reciprocal, if it is greater, the scatterer will be considered as nonreciprocal. If the scatterer is reciprocal, it can be symmetric. The characteristic parameter of the symmetry is the angle $\tau$. If it is lower than $\frac{\pi}{4}$, we will consider the scatterer as symmetric, otherwise it will be classified as asymmetric, i.e. whose the response is an helix. In the case where the scatterer is symmetric, a new classification scheme based on $\overrightarrow{S}^{sym}_{max}$ can be proposed. This classification scheme is based on the comparison of the the quantity $z$ of the matrix under study with those corresponding to the reference targets $z_{ref}$ i.e. trihedral, dihedral, dipole, cylinder, narrow-diplane and quarter wave device. In order to compare the measured $z$ and the scattering responses of the targets of reference, the following metric must be considered:

$$d(z, z_{ref}) = \frac{|1 + z^* z_{ref}|}{\sqrt{1+|z|^2}\sqrt{1+|z_{ref}|^2}} \tag{25}$$

Finally, the measured scatterer $z$ is classified according to the shortest distance $d(z, z_{ref})$.

## 4. POLARIMETRIC HYPERIMAGE CONCEPT

By applying the polarimetric Cameron decomposition to the hyper-scattering matrix (6), we obtain, on the one hand, a polarimetric evolution of the scatterers versus emitted frequency and observation angle, on the other hand a polarimetric spatial response for each frequency and angle of presentation. This defines the polarimetric hyperimage concept [9], [10].

$$[S](\overrightarrow{r}, \overrightarrow{k}) = A(\overrightarrow{r}, \overrightarrow{k}) \Big(\cos(\theta_{rec}(\overrightarrow{r}, \overrightarrow{k})) \Big(\cos(\tau(\overrightarrow{r}, \overrightarrow{k}))\,[S]^{sym}_{max}(\overrightarrow{r}, \overrightarrow{k}) + \sin(\tau(\overrightarrow{r}, \overrightarrow{k})) [S]^{sym}_{min}(\overrightarrow{r}, \overrightarrow{k})\Big) + \sin(\theta_{rec}(\overrightarrow{r}, \overrightarrow{k}))\,[S]_{nr}(\overrightarrow{r}, \overrightarrow{k})\Big) \tag{26}$$

From the cameron decomposition of the hyper-scattering matrix, we extract two polarimetric hyperimages, the huynen orientation $\psi(\overrightarrow{r}, \overrightarrow{k})$ and the classification $Classification(\overrightarrow{r}, \overrightarrow{k})$. These polarimetric hyperimages have been tested on the Cyrano weapon model and allow to describe the backscattering phenomena.

■ **Leading edges (P2,P3) :** Their directional responses in the angle-frequency fields and their polarimetric nature, dipole, express diffraction phenomena caused by the backscattering edges. Their orientation in the horizontal plane ($\theta = \pm 20$) and in the vertical plane ($\psi = \pm 10$) are perfectly found again. So, polarimetric hyperimages globally describe the backscattering phenomena (fig 4.).

■ **Trailing edges (P4,P5) :** Their directional responses in the angle-frequency fields and their polarimetric nature, dipole, express diffraction phenomena caused by the backscattering edges. Their orientation in the horizontal plane ($\theta = \pm 10$) are perfectly found again (fig 4.). The fact, that the radar does not point out the inclination in the vertical plane (upper view), explains the Huynen orientation ($\psi = \pm 90$).

■ **Wings (P6,P7) :** There are two directional polarimetric responses ($\theta = \pm 10$ and $\theta = \pm 20$). Theses responses are not

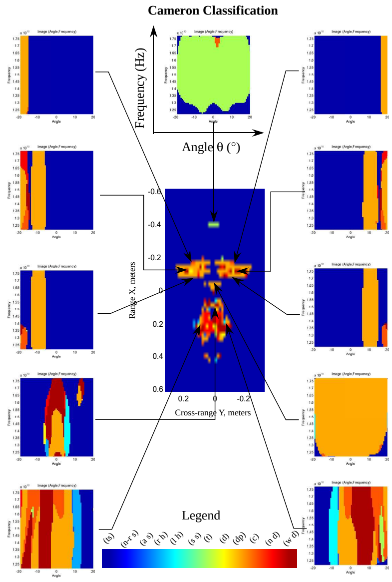


**Fig. 4**. Evolution of the polarimetric nature versus the emitted frequency and the illumination angle.

produced by the wings but they are the result of the Heisenberg incertitude. Indeed, there is a melting of polarimetric contribution between leading and trailing edges. This case, characterizes the limitations of the polarimetric hyperimages.

■ **Stabilizers (P10,P11) :** Their polarimetric response is anisotropic. Indeed, their polarimetric nature depends on the observation angle. We can explain this non-stationary behavior by the fact that radar does not see the same geometry for all angles of presentation. So, the dipole response with an orientation in the vertical plane ($\psi = \pm 45$), in the horizontal plane ($\theta \simeq 0$), is caused by the edge of the stabilizer (fig 4.).

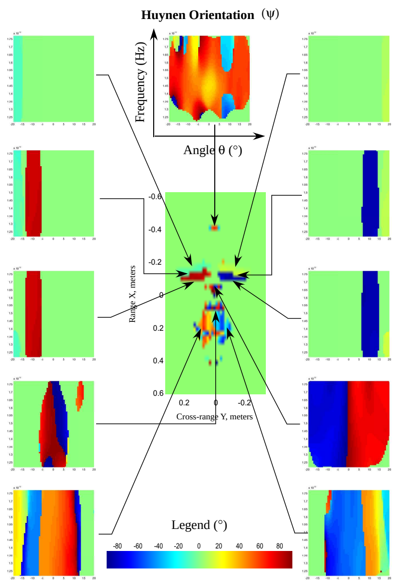


**Fig. 5**. Evolution of the Huynen orientation versus the emitted frequency and the illumination angle.

The joint use of 2D time-frequency analysis and the polarimetric Cameron decomposition, allows to build polarimetric hyperimages. These representations describe the scatterers by their nature (geometry), their relative orientation in the horizontal plane and their absolute orientation in the vertical plane. Despite the limitations caused by the Heisenberg incertitude, they give us a best understanding of backscattering mechanisms and can be an efficient tool to improve targets recognition based on physical parameters.

## 5. CHARACTERISTICS PARAMETERS

Polarimetric hyperimages are too dense information sources to be used directly for classification of scatterers. So, the aim now is to search parameters which characterize the polarimetric dispersive and anisotropic behavior. These parameters must release from the orientation to allow to classify scatterers of the same nature but with a different orientation. The first considered parameter is the entropy. Indeed the entropy can be defined from the polarimetric contributions: the maximum symmetric component, the minimum symmetric component, the nonreciprocal component (30).

$$P_1 = \frac{\cos(\theta_{rec})\cos(\tau)}{\cos(\theta_{rec})\cos(\tau) + \cos(\theta_{rec})\sin(\tau) + \sin(\theta_{rec})} \quad (27)$$

$$P_2 = \frac{\cos(\theta_{rec})\sin(\tau)}{\cos(\theta_{rec})\cos(\tau) + \cos(\theta_{rec})\sin(\tau) + \sin(\theta_{rec})} \quad (28)$$

$$P_3 = \frac{\sin(\theta_{rec})}{\cos(\theta_{rec})\cos(\tau) + \cos(\theta_{rec})\sin(\tau) + \sin(\theta_{rec})} \quad (29)$$

$$H = -\sum_i P_i \log(P_i) \quad (30)$$

A lower entropy means that one polarimetric contribution dominates the two others. A greater entropy means that the response is a melting of the three contributions.

Entropy is not a good parameter in our case (see fig 6). Indeed we work on man-made targets and this class of targets presents an important symmetry contribution. So, the entropy will be always lower. Moreover, the entropy does not release from the orientation. We must search for other parameters.

From the polarimetric hyperimage defined by multidimensional wavelet and Cameron decomposition, we extract a parameter defined by :

$$\rho_i(\overrightarrow{r}) = \frac{\sum_k Span(\overrightarrow{r}, \overrightarrow{k})\delta(class - i)}{\sum_k Span(\overrightarrow{r}, \overrightarrow{k})} \quad (31)$$

This characteristic vector is an histogram which defines an average energetic polarimetric behavior in the angular and frequency fields. If it presents a dominating component, it means that the scatterer is stationary and otherwise it is non-stationary. It seems to be a good indicator which moreover is not dependent from the orientation.

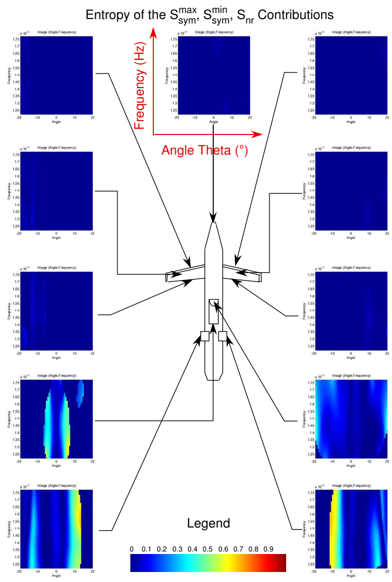


**Fig. 6**. Evolution of the entropy versus the emitted frequency and the illumination angle.

## 6. CLASSIFICATION

From this parameter we process a supervised classification. We select reference scatterers whose reference histograms define classes. Then the classification is processed by a simple euclidian distance. On the SAR image (fig 7) there are two fighters. We select on the first plane three reference scatterers, the stabilizer, the body, and the wing, whose characteristics vectors are represented on the figure 7.

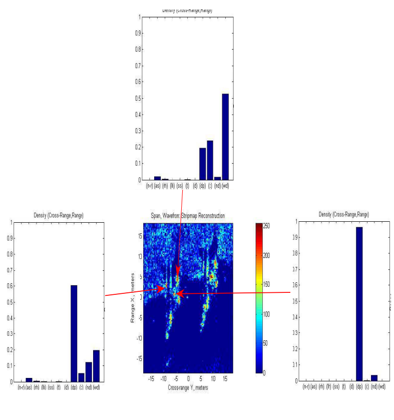

**Fig. 7**. Characteristics vectors of reference scatterers

Then a classification is made by an euclidian distance. We can see that the stabilizer and the body are identified. However, there is a confusion between the stabilizer class and the wing class for the wings. It can be explained by the fact that wings and stabilizers have a near non-stationary behavior. This classification improves the Cameron classification results which cannot distinguish between the stabilizer, the wing and the body. Cameron classification classifies the stabilizer, the wing and the body as dipole.

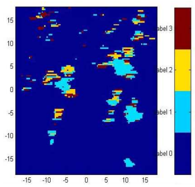

**Fig. 8**. Classification based on the anisotropic and dispersive behavior of scatterers

## 7. CONCLUSION

The joint use of multidimensional wavelet and Cameron decomposition allow to represent the polarimetric behavior of scatterers versus emitted frequency and illumination angle. The backscattering phenomena can be interpreted according to their nature, their relative orientation in the horizontal plane and their absolute orientation in the vertical plane. From these representations a characteristic parameter has been extracted to highlight the average polarimetric behavior of scatterers. A classification based on this parameter is processed by a simple euclidian distance. This classification has been tested on SAR images and allow to distinguish different structures that the Cameron decomposition cannot differentiate.

## 8. REFERENCES


[1] M. Soumekh, *Fourier Array Imaging*, Prentice Hall, Englewood Cliffs, 1994.

[2] D.L. Mensa, *High Resolution Radar Imaging*, Artech House, USA, 1981.

[3] J. Bertrand, P. Bertrand and J.P. Ovarlez, *Frequency Directivity Scanning in Laboratory Radar Imaging*, Int. J of Imaging Systems and Technology, 5, 1994, 39-51.

[4] J.P. Ovarlez, L. Vignaud, J.C. Castelli, M. Tria and M. Benidir, *Analysis of SAR Images by Multidimensional Wavelet Transform*, IEE-Radar, Sonar and Navigation, Special issue on time-frequency analysis for synthetic aperture radar and feature extraction, 150(4), august 2003, 234-241.

[5] M. Tria, J.P. Ovarlez, L. Vignaud, J. Castelli and M. Benidir *SAR Imaging Using Multidimensional Continuous Wavelet Transform*, Proc. EUSIPCO, september 2004, Vienna, Austria.

[6] S.R. Cloude and E. Pottier, *A Review of Target Decomposition Theorems in Radar Polarimetry*, IEEE trans. on geoscience and remote sensing, vol 34. num. 2, march 1996.

[7] W. L. Cameron and L. K. Leung, *Identification of Elemental Polarimetric Scatterer Responses in High-resolution ISAR and SAR Signature Measurements*, Proc. Second International Workshop on Radar Polarimetry (JIPR'1992), 8-10 september 1992, Nantes, France, 196-205.

[8] W. L. Cameron, N. N. Youssef and L. K. Leung, *Simulated Polarimetric Signatures of Primitive Geometrical Shapes*, Trans. IEEE Geosci. Remote Sensing, 34(3), may 1996, 793-803.

[9] M. Duquenoy, J.P. Ovarlez, L. Ferro-Famil, L. Vignaud and E. Pottier, *Study of Dispersive and Anisotropic Scatterers Behavior in Radar Imaging Using Time-Frequency Analysis and Polarimetric Coherent Decomposition*, Proc. IEEE Radar International conference, 24-27 april 2006, Verona, USA.

[10] M. Duquenoy, J.P. Ovarlez, L. Ferro-Famil, L. Vignaud and E. Pottier, *Study of Dispersive and Anisotropic Scatterers Behavior in Radar Imaging Using Time-Frequency Analysis and Polarimetric Coherent Decompositions.*, Proc. EUSAR conference, 16-18 may 2006, Dresden, Germany.